

BICONTINUOUS SILICA-EPOXY NANOCOMPOSITES

Charles M. D. Shaw¹, David B. Anthony², Ian Hamerton³, Milo S. P. Shaffer⁴

¹ Department of Materials, Imperial College London, London, United Kingdom, c.shaw20@imperial.ac.uk, <https://www.imperial.ac.uk/nanostructures-and-composites/people>

² Department of Chemistry, Imperial College London, London, United Kingdom, d.anthony08@imperial.ac.uk, <https://www.imperial.ac.uk/people/d.anthony08>

³ Bristol Composites Institute, University of Bristol, Bristol, United Kingdom, ian.hamerton@bristol.ac.uk, <https://research-information.bris.ac.uk/en/persons/ian-hamerton>

⁴ Department of Materials and Department of Chemistry, Imperial College London, London, UK, m.shaffer@imperial.ac.uk, <https://www.imperial.ac.uk/people/m.shaffer>

Keywords: Nanocomposite, Silica, Aerogel, Organic-Inorganic Hybrid

ABSTRACT

Monolithic mesoporous silica (silica aerogel) is presented as 3D continuous reinforcement for conventional thermoplastic matrices. Backfilling of the porous silica network with epoxy resin yields a bicontinuous material with interlocking silica and epoxy phases. Long range connectivity in the resulting silica reinforcement will better facilitate load transfer within the nanocomposite whilst ensuring uniform silica dispersion. This reinforcing structure may increase stiffness whilst retaining the toughness of the epoxy resin. A stiffer matrix will better resist fibre micro-buckling when applied to unidirectional fibre composite materials leading to an overall improvement in compressive strength. A pre-formed monolithic reinforcement avoids the undesirable viscosity and agglomeration effects seen for dispersed nanoparticulate fillers allowing potentially higher weight loadings of silica reinforcement. Silica content is instead limited only by the ability of the porous silica aerogel network to uptake epoxy resin. Therefore, a mesoporous silica precursor of high envelope density ($> 0.2 \text{ g.cm}^{-3}$) with a sufficiently open pore structure for epoxy-backfilling is required.

1 INTRODUCTION

Epoxy resins are a popular choice for structural composite matrices due to their ease of processing and excellent mechanical properties in a range of environments. However, their stiffness is lower than some high-performance thermoplastics and much lower than inorganic materials. Well-dispersed nanofillers can improve the elastic moduli of epoxies without reducing toughness [1]. However, discontinuous particles do not fully exploit the intrinsic properties of the reinforcement and may complicate processing through increased resin viscosity [2]. Uneven filler dispersion resulting from particle agglomeration and self-filtration may occur at high filler loadings resulting in the formation of stress-concentrating sites [3-4]. A fully connected, bicontinuous, reinforcing structure may offer a more effective way to increase stiffness, by providing a direct path for load transfer and potentially a high filler fraction. Such a structure can be fabricated by infusing a porous silica monolith with epoxy resin. This inorganic-organic hybrid potentially provides a bicontinuous structure in which the beneficial material properties of each phase (stiff silica and tough epoxy) may be better exploited. The inorganic reinforcing skeleton improves load transfer whilst additional failure modes associated with nanoscale reinforcement may help to retain toughness [5]. In a recent publication such a material was employed as matrix in a glass fibre reinforced composite leading to improvements in composite compressive strength and interlaminar shear strength [6]. Continuous silica networks can be prepared via low temperature sol-gel process developed for aerogel technologies. Conventional silica aerogels are

generally formed at very low densities ($< 0.1 \text{ g.cm}^{-3}$) and used for their low thermal conductivity. The low density and the fragility of the connections between primary particles results in a weak, brittle material. Crosslinking the silica particles with organic polymers to produce an X-aerogel, without complete pore filling, can improve properties whilst maintaining a low density [7]. The microstructures of these two classes of silica-epoxy nanocomposites, discontinuous particle filled resin and polymer modified aerogel, are shown pictorially in Figure 1. In this work, our goal was to use the 3D connectivity of an aerogel as a reinforcement to produce a bicontinuous composite with greater stiffness and similar toughness to unreinforced epoxy. Unlike typical aerogel synthesis, therefore, we aimed to form bicontinuous silica networks at relatively high densities, retaining sufficient porosity to allow full infusion with epoxy. Herein, 3D aerogel monoliths are infused with a commercially available structural epoxy resin to produce samples compatible with standardised mechanical testing procedures. We describe the silica pre-form synthesis, the epoxy infusion under vacuum, and the fabrication of samples for measurement of mechanical and thermal properties.

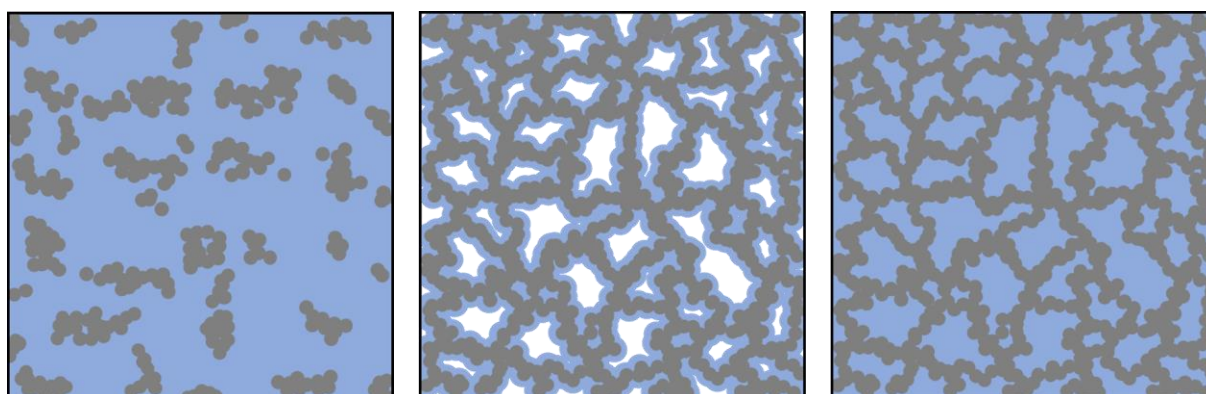


Figure 1: Cartoons depicting the microstructures of epoxy-silica nanocomposites. Left: Epoxy resin (blue) reinforced with powdered silica aerogel (grey). Centre: Epoxy-crosslinked silica X-aerogel (grey aerogel with blue crosslinking). Right: Bicontinuous silica-epoxy hybrid monolith (grey aerogel and blue epoxy).

2 EXPERIMENTAL

2.1 CHEMICAL REAGENTS

For the synthesis of silica aerogel monoliths tetramethylorthosilicate (98%, TMOS) and chlorotrimethylsilane ($\geq 98\%$, TMCS) were purchased from Sigma Aldrich (GB), and acetone (technical grade), ethanol (absolute), water (HPLC grade), and *n*-hexane (dehydrated) were purchased from VWR (GB). An epoxy resin with its associated hardener (Gurit Prime 27 epoxy resin and Prime Extra Slow hardener, Marineware Ltd., GB) were infused into the silica aerogel monoliths to produce silica-epoxy bicontinuous composites. The epoxy and hardener were mixed according to manufacturer's instructions and degassed before use. All chemicals were used as received.

2.2 SILICA AEROGEL SYNTHESIS AND CHARACTERISATION

Silica aerogel monoliths were produced by combining water, TMOS and ethanol in a molar ratio of 24:1:1.8. This mixture was stirred for 1 h at 25 °C to give a single transparent sol phase which was then poured into a mould. Solid cylinder (6 mm diameter) and flat plate (20 mm x 20 mm) aerogel samples were cast in moulds made by machining 20 mm thick high-density polyethylene (HDPE) sheet (PE 300, Direct Plastics, GB) on an XYZ CNC router (CA). Gelled samples were aged for 4 days at 25 °C to ensure complete reaction before exchanging from residual solvent to ethanol. Hydrophobisation of the silica surface was performed by immersion in a TMCS:*n*-hexane:ethanol mixture (1:1:8 ratio by

volume). Samples were then exchanged back to ethanol before a final exchange to acetone over 3 days. Finally, samples were dried from supercritical CO₂ using a Leica EM CPD300 critical point dryer (DE). Envelope densities were determined by Archimedes' balance method in de-ionised water (. Skeletal density was determined by helium pycnometry (Micrometrics AccuPyc II 1340, GB). Specific surface area, pore volume, and pore radius distributions were determined from gas sorption isotherms (N₂) using a Quantachrome NOVAtouch gas sorption analyser (US).

2.3 INFUSION OF EPOXY RESIN INTO SILICA AEROGEL NETWORK TO PRODUCE BICONTINUOUS NANOCOMPOSITES

Monolithic silica aerogel solid cylinders (diameter \approx 6 mm, length \approx 15 mm) and flat plates (\approx 40 mm x 40 mm x 3 mm) were backfilled with epoxy by immersion in degassed epoxy resin/hardener mixture under reduced pressure in a Memmert VO400 (DE) vacuum oven. The chosen commercially available resin system has low viscosity (170 cP to 180 cP at 25 °C) and long vacuum flow time (7 h 40 min at 25 °C). Once immersed, the entire system was evacuated to 1 mbar in a vacuum oven for 6 h at 22.5 °C. Samples were then removed from the liquid resin and excess resin was allowed to run off. Curing was completed in accordance with the manufacturer's stated cure cycle of 24 h at 25 °C followed by a post-cure of 16 h at 50 °C.

2.4 CHARACTERISATION OF BICONTINUOUS COMPOSITE STRUCTURE

The degree of infusion of epoxy into the porous silica structure was quantified as a backfill volume percentage (β) using Equation (1). $\Delta\rho_b$ is the difference in envelope density between the unmodified silica aerogel monolith and the epoxy-infused silica aerogel monolith, φ is the porosity of the silica aerogel monolith, and ρ_e is the cured epoxy density determined by Archimedes' balance method. Porosity was determined from skeletal and envelope densities (Equation (2)). The change in morphology following epoxy backfilling was observed by scanning electron microscopy using a LEO Gemini 1525 field emission gun scanning electron microscope (SEM) with an accelerating voltage of 5 kV with In-lens detector. The homogeneity of the silica distribution in the bicontinuous nanocomposite was measured by energy dispersive X-ray analysis (EDX) using a grid pattern of 20 points with 5 μ m spacing at each of 3 sites of interest.

$$\beta = \frac{\Delta\rho_b}{\varphi \cdot \rho_s} \quad (1)$$

$$\varphi = 1 - \frac{\rho_b}{\rho_s} \quad (2)$$

2.4 MEASUREMENT OF COMPRESSIVE PROPERTIES

Compression test specimens were prepared from 6 mm diameter solid bicontinuous nanocomposite cylinders and baseline epoxy cylinders. These rough cylinders were machined to 1:1 cylinders (5.5 mm x 5.5 mm) using a manual lathe. Test specimens were painted with a stochastic pattern for digital image correlation (DIC) strain analysis (Images captured using LaVision Stereo DIC with two 16-megapixel, imager E-lite stereo cameras. Images processed using LaVision DaVis 10). Compressive properties were measured on an Instron 8872 Universal Testing Machine(US) fitted with a 10 kN load cell. A modified ASTM D695 testing procedure was employed [8]. Specimens were subjected to a 10 N pre-load before quasi-static loading at a rate of 0.006 mm.s⁻¹ to a maximum load of 9.5 kN. PTFE tape was applied to the testing platens to decrease friction for prevention of sample barreling. Strain measurements were made by 3D digital imaged correlation with a capture rate of 1 s⁻¹. Compression modulus was measured from the gradient of the plot of true compression stress against true compression strain in the range of 0.3 % to 1.0 % strain. True strain and true stress were calculated from the DIC output strains ϵ_{xx} and ϵ_{yy} using Equation (3) and Equation (4) respectively where F is the applied load and A_0 is the initial cross-sectional area of the sample perpendicular to the applied load.

$$\varepsilon_t = -\ln(1 + \varepsilon_{yy}) \quad (3)$$

$$\sigma_t = F/[A_0 \cdot (1 + \varepsilon_{xx})^2] \quad (4)$$

2.5 THERMAL CONDUCTIVITY MEASUREMENT

Flat plate bicontinuous nanocomposite and baseline epoxy samples and were polished to a thickness of 2 mm and finished with diamond polishing compound (3 μm particle size). 8 mm x 8 mm x 2 mm rectangular prismatic specimens were cut and then coated with a conductive graphite coating (Graphit 33, Kontakt Chemie, DE). Thermal diffusivity was measured by light flash method using a LFA 447 Nanoflash Light Flash System (Netzsch, DE) in accordance with ASTM E1461 [9]. Thermal conductivity was calculated from thermal diffusivity, density, and specific heat capacity (Equation (8)).

$$\lambda(T) = \alpha(t) \cdot \rho(T) \cdot c_p(T) \quad (5)$$

2.6 DIFFERENTIAL SCANNING CALORIMETRY

Differential scanning calorimetry (DSC) was used to determine the effect of the continuous silica reinforcement on the degree of cure of the epoxy resin. Normalised heat flow was measured in the range of $-50\text{ }^\circ\text{C}$ to $150\text{ }^\circ\text{C}$ using a TA Q2000 DSC (TA Instruments, GB). Glass transition temperature (T_g) and specific heat capacity (C_p) values were extracted from this data using TRIOS software (TA Instruments, GB). Specimens (of mass in the range of 2 mg to 6 mg) were held in sealed aluminium pans of known mass, heat flow was measured relative to an empty reference pan of known mass.

3 RESULTS AND DISCUSSION

3.1 SYNTHESIS OF BICONTINUOUS SILICA – EPOXY NANOCOMPOSITE

3.1.1 SILICA AEROGEL REINFORCING SKELETON

The bicontinuous silica-epoxy nanocomposite was produced in two stages: synthesis of a continuous silica reinforcement (monolithic silica aerogel) followed by complete backfilling of silica aerogel with epoxy resin. Consequently, the silica aerogel phase requires a pore structure with sufficient pore size and interconnectivity to allow liquid epoxy resin to fully infiltrate the structure. However, in order to maximise the reinforcing contribution of the silica phase, aerogel of unusually high envelope density was sought. All aerogel samples formed were functionalised with trimethylchlorosilane (TMCS) for the following reasons:

- Hydrophilic (non TMCS-treated) samples formed in this work were found to fracture in the presence of ambient moisture.
- Hydrogen bonded water molecules would be difficult to remove ahead of epoxy infusion. This residual water could affect the epoxy cure and produce voids in the composite structure.
- Functionalisation with trimethylsilyl groups prevents silanol groups from reacting chemically with epoxy resin or hardener. This reaction may alter the stoichiometry of the epoxy resin/hardener mixture. Silica-epoxy bi-continuous materials with a designed covalent interface will nevertheless be explored in future work.

A sol-gel precursor consisting of only tetramethylorthosilicate (TMOS) and de-ionised water was chosen to simplify the evaluation of a suitable aerogel density for epoxy-backfilling. TMOS and water can react and self-mix without additional solvent or catalyst. This unlimited miscibility means that the

upper limit for aerogel density is the requirement for a 2:1 water:TMOS stoichiometric ratio [10]. In-contrast, the density of samples formed from tetraethylorthosilicate (TEOS) is limited by the requirement for a co-solvent as it is fully immiscible with water. The greater miscibility of TMOS with water allows the formation of a broader range of aerogel densities aided the investigation of a suitable silica content in the bicontinuous network. This investigation yielded a silica aerogel of 0.23 g.cm^{-3} as a suitable candidate reinforcing skeleton. This composition was the densest aerogel in the systematic study that was able to be fully backfilled with epoxy resin at a scale suitable for evaluation of bulk mechanical properties. BJH pore radius data for this composition indicates that for hydrophobised silica aerogel indicates that minimum pore radii in the range of 2 nm to 3 nm are required for successful epoxy infusion. Physical properties of the chosen silica aerogel reinforcing network are summarised in Table 1. The skeletal density value of 1.40 g.cm^{-3} is lower than that of amorphous silica due to the presence of the low-density hydrophobic coating.

ρ_b (g.cm^{-3})	ρ_s (g.cm^{-3})	SSA ($\text{m}^2.\text{g}^{-1}$)	r_{pore} (nm)	V_{pore} ($\text{cm}^3.\text{g}^{-1}$)
0.226 ± 0.009	1.40 ± 0.01	951 ± 25	2.60 ± 0.17	3.81 ± 0.25

Table 1: Silica aerogel monolith properties where ρ_b is envelope density, ρ_s is skeletal density, SSA is specific surface area, r_{pore} is mean pore radius and V_{pore} is pore volume. Uncertainty is given as one standard deviation.

3.1.2 BACKFILLING SILICA AEROGEL WITH EPOXY RESIN TO PRODUCE A BICONTINUOUS NETWORK

Bicontinuous nanocomposite specimens were produced from silica aerogel monoliths of geometries suitable for mechanical testing. Rods ($\phi \approx 6 \text{ mm}$, $l \approx 15 \text{ mm}$) were cast for compression test samples and flat plates ($40 \text{ mm} \times 40 \text{ mm} \times 3 \text{ mm}$) were cast for thermal conductivity analysis. The porous aerogel structure was backfilled with epoxy resin by immersing the dry aerogel monolith in mixed, degassed epoxy resin-hardener mix (Figure 2).

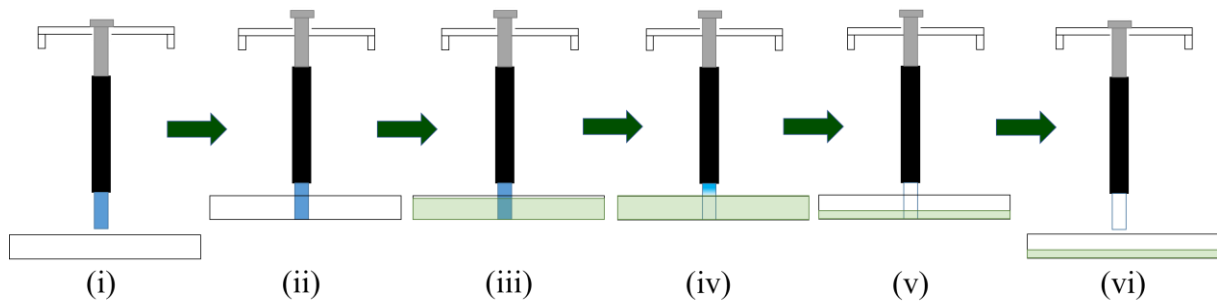


Figure 2: Procedure for infusion of epoxy resin into silica aerogel monolith. (i) Silica aerogel cylinder (blue) is held in heat-shrink tubing (blue) and suspended over a vessel in a manner which allows free upward movement but restricted downward movement. (ii) Vessel is raised to provide upward support to silica aerogel cylinder. (iii) Degassed epoxy resin-hardener mix is added to vessel. (iv) System is evacuated. (v) After 4 h increased transparency is observed, system is vented to air. (vi) Vessel is lowered to remove silica aerogel.

Successful displacement of air by epoxy resin was observed through evolution of bubbles and a change in appearance of the aerogel from a translucent bluish colour (a result of Rayleigh scattering by the porous structure) to first opaque white before a final transparent, colourless appearance. The increased transparency is a result of improved refractive index matching and a reduction in scattering. Samples were post-cured in accordance with the epoxy resin specification before machining to the desired specimen geometries (Figure 3).

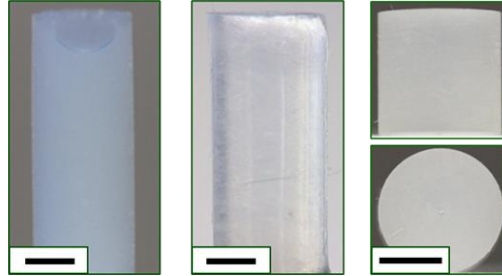


Figure 3: Silica aerogel cylindrical monolith. Centre: Bicontinuous silica-epoxy nanocomposite. Right: Bicontinuous silica-epoxy nanocomposite compression test sample side view (upper) and end view (lower). Scale bar = 3 mm.

Density measurements show that backfilling of the porous structure with epoxy resin is near complete (Table 2). The reinforcing skeleton in the nanocomposite accounts for 19 % of the composite by mass, going forward this material will be referred to as NC19 (19 wt.% reinforcement bicontinuous nanocomposite) and its aerogel precursor is named SAG19.

ρ_f (g.cm ⁻³)	Backfill vol.%	Void vol.%	Silica wt.%	Epoxy wt.%
1.18 ± 0.01	99.9 ± 1.9	0.1 ± 1.9	18.9 ± 0.7	81.1 ± 0.7

Table 2: Summary of composition of bicontinuous silica-epoxy material. Uncertainty is given as one standard deviation.

Electron micrographs for SAG19 and NC19 show the porous aerogel before and after filling with resin (Figure 4a). Analysis of the elemental content of the bicontinuous network show that the carbon:silicon ratio varies by less than ± 2.5 % (Figure 4b). This value is within the typical experimental error for SEM EDX analysis showing that, as expected, the silica reinforcement is homogeneously distributed throughout the nanocomposite [11]. This uniformity is typically difficult to achieve at comparable silica loadings for dispersed powdered nanofillers due to high viscosity and particle agglomeration. Composites formed from powdered silica aerogel usually employ less than 5 wt.% silica for this reason [1]. Higher silica loadings are possible by use of pre-dispersed nanofiller systems [12] however these still provide processing challenges due to high viscosity which inhibits mixing and degassing.

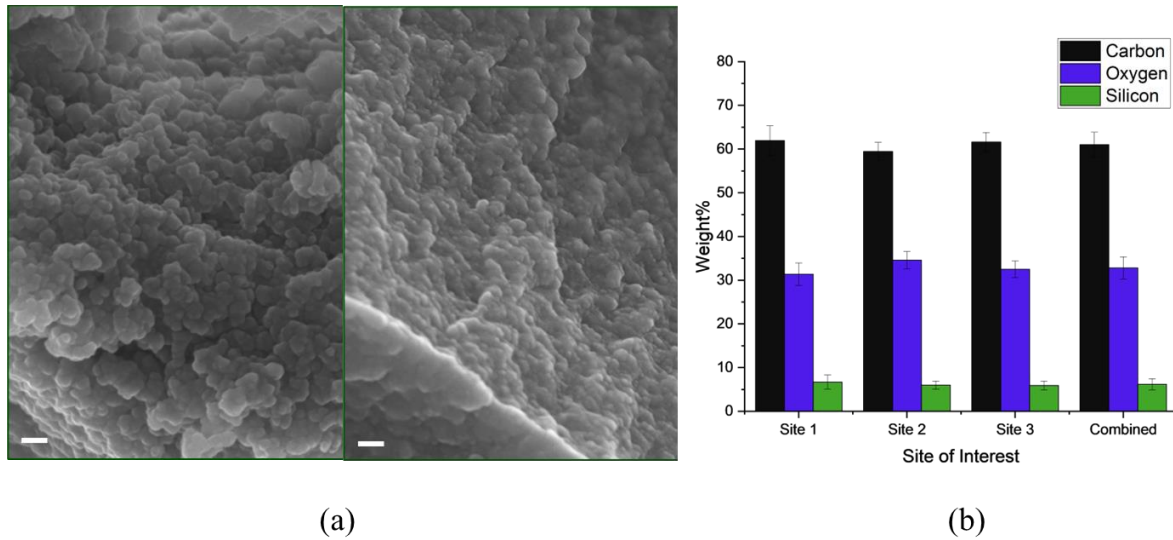


Figure 4: (a) SEM micrographs showing silica aerogel (SAG19) before (left) and after (NC19) backfilling with epoxy resin. Scale bar = 100 nm. (b) Elemental composition determined by SEM EDX of NC19 as an average of 25 measurements at each of 3 sites and overall average composition.

3.2 MECHANICAL PROPERTIES

Bicontinuous silica-epoxy nanocomposite (NC19) samples were machined to test specimen geometries as described in Section 2.4 and Section 2.5. These were tested alongside baseline epoxy resin specimens. NC19 exhibited a 26 % improvement in compression modulus over the baseline epoxy resin at a cost of only 3.5 % greater density (Table 3). This result compares favourably with nanocomposites formed with NANOPOX® where a 19 % increase in compression modulus over epoxy baseline was reported at an equivalent silica loading [12]. This improved performance is attributed to better load transfer resulting from the connectivity of the silica reinforcement in the bicontinuous nanocomposite.

Sample	Density (g.cm ⁻³)	Peak Compression Stress (MPa)	Compression Modulus (GPa)
ER	1.14	96.5 ± 2.9	3.53 ± 0.17
NC19	1.18 ± 0.01	93.9 ± 2.6	4.45 ± 0.30

Table 3: Compressive properties 19 wt.% reinforcement bicontinuous nanocomposite (NC19) and epoxy resin baseline (ER).

3.3 THERMAL PROPERTIES

Differential scanning calorimetry (DSC) data indicates a slight decrease in the glass transition temperature of the epoxy resin in the bicontinuous nanocomposite compared to epoxy resin baseline samples (Table 4). This is attributed to the non-reactive methylated surface of the silica reinforcement which results in decreased epoxy resin crosslink density at the silica-epoxy interface. In future work this deficit may be recovered by altering the silica aerogel surface treatment to introduce reactive groups to form covalent linkages at the interface. This may also improve load transfer between the two phases, enhancing the mechanical properties of the nanocomposite. Specific heat capacity (C_p) values measured by DSC were combined with thermal diffusivity (α) measurements to determine the effect of the

bicontinuous network on the thermal conductivity of the nanocomposite relative to baseline epoxy resin. These results show a 65 % decrease in the thermal conductivity (κ) when the continuous silica reinforcement is present compared to the epoxy resin baseline. This decrease is a consequence of the large difference in thermal impedance between the two phases (silica and epoxy) in conjunction with the large number of interfaces present in the bicontinuous structure.

Sample	T_g (°C)	C_p (kJ.kg ⁻¹ .K ⁻¹)	α (mm ² .s ⁻¹)	κ (W.m ⁻¹ .K ⁻¹)
ER	72.2 ± 1.7	0.95 ± 0.03	0.20 ± 0.02	0.20 ± 0.02
NC19	67.7 ± 1.0	0.39 ± 0.1	0.16 ± 0.00	0.07 ± 0.01

Table 4: Thermal properties of 19 wt.% reinforcement bicontinuous nanocomposite (NC19) and epoxy resin baseline (ER).

4 CONCLUSIONS

A nanocomposite has been synthesised in which a continuous silica network acts to reinforce a conventional commercial epoxy resin by forming a bicontinuous network. This organic-inorganic hybrid displays improved compression performance over existing discontinuously reinforced systems. This, combined with processing advantages (lower viscosity, inherently uniform distribution of reinforcement) makes such materials suitable candidates for application as matrix for fibre-reinforced composites. Thermal analysis indicates that further improvement may be attained through optimisation of the epoxy-silica interface to enhance epoxy cure properties and provide more coherent load transfer between the two phases. Future studies of energy absorption in failure will investigate whether this unique material is able to deliver improved stiffness without sacrificing toughness.

ACKNOWLEDGEMENTS

The authors kindly acknowledge the funding for this research provided by UK Engineering and Physical Sciences Research Council (EPSRC) programme Grant EP/T011653/1, Next Generation Fibre-Reinforced Composites: a Full Scale Redesign for Compression a collaboration between University of Bristol and Imperial College London.

REFERENCES

- [1] S. Salimian and A. Zadhoush. Water-glass based silica aerogel: unique nanostructured filler for epoxy nanocomposites. *Journal of Porous Materials*, **26**, 2019, pp. 1755-65 (doi: 10.1007/s10934-019-00757-3).
- [2] S.S. Rahatekar, K.K.K. Koziol, S.A. Butler, J.A. Elliot, M.S.P. Shaffer, M.R. Mackley and H.A. Windle. Optical microstructure and viscosity enhancement for an epoxy resin matrix containing multiwall carbon nanotubes. *Journal of Rheology*, **50**, 2006, pp. 599-610 (doi: 10.1122/1.2221699).
- [3] M.D. Haw. Jamming, two-fluid behaviour and “self-filtration” in concentrated particulate suspensions. *Physical Review Letters*, **92** (18), 2004, Article 185506 (doi: 10.1103/PhysRevLett.92.185506).
- [4] Y. Zare, K.Y. Rhee and D. Hui. Influences of nanoparticles aggregation/agglomeration on the interfacial/interphase and tensile properties of nanocomposites. *Composites Part B: Engineering*, **122**, 2017 pp. 41-46 (doi: 10.1016/j.compositesb.2017.04.008)
- [5] M. Quaresimin, K. Schulte, M. Zappalorto and S. Chandrasekaran. Toughening mechanisms in polymer nanocomposites: From experiments to modelling. *Composite Science and Technology*, **123**, 2016, pp. 187-204 (doi: 10.1016/j.compscitech.2015.11.027)

- [6] D.B. Anthony, S. Nguyen, H. Qian, S. Xu, C.M.D. Shaw, E.S. Greenhalgh, A. Bismarck and M.S.P. Shaffer. Silica aerogel infused hierarchical glass fiber polymer composites. *Composites Communications*, **39**, Article 101531, 2023, pp. 1-9 (doi:10.1016/j.coco.2023.101531).
- [7] M.A.B. Meador, E.F. Fabrizio, F. Ilhan, A. Dass, G. Zhang, P. Vassilaras, J.C. Johnston and N. Leventis. Cross-linking amine-Modified silica aerogels with epoxies: Mechanically strong lightweight porous materials. *Chemistry of Materials*, **17**, 2005, pp. 1085-98 (doi: 10.1021/cm048063u).
- [8] ASTM International. *D695-15 Standard Test Method for Compressive Properties of Rigid Plastics*. West Conshohocken, Pennsylvania, 2015 (doi: 10.1520/D0695-15).
- [9] ASTM International. *E1461-13 Standard Test Method for Thermal Diffusivity by the Flash Method*. West Conshohocken, Pennsylvania, 2022 (doi: 10.1520/E1461-13R22).
- [10] K. Kajihara. Recent advances in sol-gel synthesis of monolithic silica and silica-based glasses. *Journal of Asian Ceramic Societies*, **1** (2), 2013, pp.121-133 (doi: 10.1016/j.jascer.2013.04.002).
- [11] R.A. Carlton, C.E. Lyman and J.E. Roberts. Accuracy and precision of quantitative energy-dispersive X-ray spectrometry in the environmental scanning electron microscope. *Scanning*, **26** (4), 2004, pp. 167-74 (doi: 10.1002/sca.4950260404).
- [12] F. Liu, S. Deng and J. Zhang. Mechanical properties of epoxy and its carbon-fibre composites modified by nanoparticles, *Journal of Nanomaterials*, **2017**, Article 8146248, 2017, pp. 1-9 (doi: 10.1155/2017/8146248).